The PI3K regulatory subunits p55α and p50α regulate cell death *in vivo*

S Pensa[1], K Neoh[1], HK Resemann[1], PA Kreuzaler[1,2], K Abell[1,3], NJ Clarke[4], T Reinheckel[5], CR Kahn[6] and CJ Watson*,[1]

The phosphatidylinositol 3-kinase (PI3K) regulatory subunits p55α and p50α are coordinately transcriptionally upregulated by signal transducer and activator of transcription 3 (Stat3) at the onset of mammary gland involution, a process that requires Stat3. Deletion of both p55α and p50α subunits *in vivo* abrogated mammary epithelial cell death during involution. This was associated also with reduced cytosolic levels and activity of the cysteine protease cathepsin L, which is implicated in lysosomal-mediated programmed cell death (LM-PCD) and is upregulated in involution. Furthermore, involution is delayed in cathepsin L-deficient mice suggesting that the p55α/p50α subunits mediate cell death in part by elevating the level of cathepsin L resulting in increased cytosolic activity. Surprisingly, we found that p55α/p50α localize to the nucleus where they bind to chromatin and regulate transcription of a subset of inflammatory/acute phase genes that are also Stat3 targets. Our findings reveal a novel role for these PI3K regulatory subunits as regulators of LM-PCD *in vivo*.

The class IA phosphatidylinositol 3-kinases (PI3Ks) are heterodimeric enzymes that comprise a p110 catalytic subunit (p110α, p110β or p110δ) and a regulatory subunit (p85α, p85β, p55α, p55γ or p50α).[1] A single gene, *pik3r1*, encodes p85α, p55α and p50α and all three subunits share a common carboxy-terminal domain, which encompasses the p110 subunit binding site, a proline-rich region and two Src homology 2 (SH2) domains, which bind to a plethora of proteins including receptor tyrosine kinases and ankyrin3.[2] The unique amino terminal sequence of p85α comprises a Src homology 3 (SH3) and a breakpoint cluster region-homology domain, which bind to the negative regulator of PI3K, phosphatase and tensin homolog enhancing its lipid phosphatase activity.[3] The p85α subunit binds also to Rab5 and other proteins including dynamin and Grb2,[2] and can interact with X-box-binding protein-1 (XBP-1), a transcriptional mediator of the unfolded protein response (UPR), to enhance nuclear accumulation of XBP-1s in an endoplasmic reticulum (ER) stress-dependent manner.[4,5] The p55α and p50α subunits have much smaller unique N-terminal sequences of 34aa for p55α and 6aa for p50α. Specific ablation of these subunits by deleting exons 1B (p50α) and 1C (p55α) results in improved insulin sensitivity and protection from obesity-induced insulin resistance.[6] However, although p55α has been shown to bind to tubulin,[7] the function of these subunits is still somewhat enigmatic.

Involution can be divided into two phases, the first of which is reversible.[8] In the mouse, this reversible phase persists for approximately 48 h and thereafter tissue remodeling occurs,

precluding re-initiation of lactation. Gene expression analyses revealed an unexpected role for inflammatory regulators and the acute phase response (APR) during involution, reflecting the extensive tissue remodeling that occurs simultaneously with epithelial cell death.[9–11] We have shown previously that cell death during first phase involution is mediated by signal transducer and activator of transcription 3 (Stat3) regulated lysosomal membrane permeabilization and is independent of executioner caspases.[12] Furthermore, the lysosomal cathepsins B and L are strikingly upregulated during involution in a Stat3-dependent manner and leak from lysosomes to initiate cell death. Thus, Stat3 is a master regulator of the involution process.

We demonstrated previously that transcription of p55α and p50α is specifically and markedly upregulated by Stat3 at the onset of involution[13] and in a mammary epithelial cell line;[14] and this prompted us to investigate their role in mediating the Stat3 signal during the involution process. Using mice in which the unique exons encoding the amino-termini of p55α and p50α were deleted, we found that mammary gland development occurred normally until involution, when cell death was markedly reduced. The cysteine protease cathepsin L, which is implicated in lysosomal-mediated programmed cell death (LM-PCD), is rapidly upregulated in involution, although reduced cytosolic levels and activity are found in $p55α^{−/−}/p50α^{−/−}$ glands. Furthermore, cathepsin L-deficient mice exhibited delayed involution suggesting that the p55α/p50α subunits mediate cell death in part by elevating cathepsin L activity. Interestingly, p55α/p50α localize to the nuclei of

[1]Department of Pathology, University of Cambridge, Cambridge, UK; [2]Department of Biochemistry, University of Cambridge, Cambridge, UK; [3]LEO Pharma A/S Industriparken 55, Ballerup, Denmark; [4]GlaxoSmithKline, Stevenage, UK; [5]Institute of Molecular Medicine and Cell Research and BIOSS Centre for Biological Signalling Studies, Albert-Ludwigs-University Freiburg, Freiburg, Germany and [6]Joslin Diabetes Center, Boston, MA, USA
*Corresponding author: CJ Watson, Department of Pathology, University of Cambridge, Tennis Court Road, Cambridge CB2 1QP, UK. Tel: +44 0 1223 333725; Fax: +44 0 1223 333346; E-mail: cjw53@cam.ac.uk

Abbreviations: LM-PCD, lysosomal-mediated programmed cell death; PI3Ks, phosphatidylinositol 3-kinases; SH2, Src homology 2; SH3, Src homology 3; XBP-1, X-box-binding protein-1; UPR, unfolded protein response; ER, endoplasmic reticulum; Stat3, signal transducer and activator of transcription; APR, acute phase response

involuting epithelial cells and regulate transcription of a number of genes including some Stat3 target genes.

Results

p55α/p50α regulate cell death *in vivo*. Examination of mammary glands from mice deficient in both p55α and p50α, but replete for p85α, revealed a striking delay in involution (Figures 1a and b). This was associated with delayed tissue remodeling, as shown by the quantification of the area occupied by adipocytes, which is significantly reduced at 48 and 72 h of involution (Figure 1c). In addition, 24-h involution samples show a 12-fold reduction in the number of detached dying cells (Figures 1b and d), also indicated by decreased cleaved caspase 3 levels (Figures 1e and f). Levels of p-Akt and phospho-glycogen synthase kinase 3 β were similar between control and knockout mice except at 72-h involution (Supplementary Figure 1a) due largely to the presence of Akt2 in the adipose tissue at this time point (Supplementary Figures 1b and c). Thus, the role of p55α/p50α during involution is likely independent of PI3K catalytic activity. This suggests that these subunits have a role in regulating cell death during involution by some other mechanism. Notably, p55α/p50α expression in the mammary gland seems to be restricted to the epithelium and is not found in the adipose compartment (Supplementary Figure 1c).

p55α/p50α regulate cathepsin L expression and cytosolic activity. We have shown previously that, during involution, Stat3 upregulates expression of the lysosomal proteases cathepsins B and L while downregulating expression of the endogenous cathepsin inhibitor Spi2a.[12] Importantly, as opposed to cathepsin B, which shows a modest 4-fold increase at the onset of involution (Kreuzaler *et al.*[12] and Figure 3d), cathepsin L shows a striking induction within 24-h involution, as shown by immunofluorescence staining and a corresponding 22-fold induction at the mRNA level (Figures 2a and 3d; Kreuzaler *et al.*[12] and Burke *et al.*[15]). We confirmed that cathepsin L localizes to vesicles at 24-h involution using immunofluorescence microscopy (Figure 2a). The discrete puncta observed become more diffuse as involution progresses and begin to disappear altogether at 96 h, reflecting the reduction in cathepsin L compared with cathepsin B at this time point.[12] Interestingly we found that, while both cathepsins B and L normally colocalized, a proportion of the cathepsin L-positive vesicles did not contain cathepsin B (Figure 2b and Supplementary Figure 2) suggesting that there may be an alternative transport system that delivers cathepsin L to discrete vesicles. Importantly, ablation of p55α/p50α affected primarily cathepsin L levels, which were markedly reduced in knockout tissue and this was particularly marked in the extent of cathepsin L leakage to the cytosol (Figure 2c and Supplementary Figure 3a). In contrast, cathepsin B levels were relatively unchanged (Supplementary Figures 3b–d). This was reflected in enzymatic activity assays on both lysosomal and cytosolic extracts, showing reduced cathepsin L cytosolic activity both at 24- and 48-h involution (Figure 2d). As cathepsin B activity is unaffected by p55α/p50α ablation, this suggests that lysosomal leakiness is unlikely to be perturbed. Therefore, the reduced cytosolic activity of cathepsin L most likely reflects the reduced protein levels observed.

We have previously shown that the mitochondrial pathway of cell death is downstream of LM-PCD and is executioner caspase independent.[12] Nevertheless, we investigated whether deletion of p55α/p50α affected components of the mitochondrial pathway. Thus, we analyzed the expression of the pro-apoptotic Bcl-2 family members Bax and Bid and the anti-apoptotic factors Bcl-2 and Bcl-xL (Supplementary Figure 4a). No major changes were observed, although slightly reduced cytosolic levels of cytochrome c were apparent at 48-h involution in the $p55\alpha^{-/-}/p50\alpha^{-/-}$ glands (Supplementary Figure 4b), suggesting an impact of cathepsin L on the mitochondria.

p55α/p50α regulate gene expression at the transcriptional and post-transcriptional level. Recently, p85α has been shown to interact with XBP-1 and regulate its nuclear translocation and transcriptional activity.[4,5] We therefore sought to determine if p55α/p50α could exert a similar function on the master regulator of involution, Stat3. Analysis of total and nuclear extracts of $p55\alpha^{-/-}/p50\alpha^{-/-}$ glands at different involution time points revealed no difference in the induction of Stat3 phosphorylation or on its translocation to the nucleus (Supplementary Figures 5a–c). Nuclear localization of p85α and p85β has been described in different cellular systems.[4,16,17] To determine if the regulatory subunits localize to the nuclei of mammary cells, we analyzed nuclear and cytosolic extracts of a number of involution time points. Interestingly, we detected nuclear p85α at 10 days lactation, while p55α and p50α exhibited nuclear localization immediately upon their expression at the onset of involution (Figure 3a). Further analysis of nuclear compartments revealed an association of all three regulatory subunits, and phospho-Stat3 (p-Stat3), with chromatin-enriched extracts of EpH4 mammary epithelial cells, suggesting either a direct or indirect role in regulating transcription (Figure 3b). This prompted us to carry out a microarray analysis of control and $p55\alpha^{-/-}/p50\alpha^{-/-}$ mammary glands at 24 h of involution. A number of genes were either upregulated or downregulated in the $p55\alpha^{-/-}/p50\alpha^{-/-}$ glands (Supplementary Tables 1 and 2, respectively) and a subset of these was validated by QRT-PCR (Figure 3c). Interestingly, a number of these genes are associated with cell migration and tissue remodeling and the APR. Although osteopontin (Spp1), SAA2 and Tlr2 are expressed at higher levels in the absence of p55α/p50α, Slpi and synaptopodin are suppressed in p55α/p50α-deficient glands. Many of the genes identified in the microarray have previously been shown to be Stat3 targets (Hughes *et al.*,[10] Supplementary Table 3 and CJW, unpublished). This suggests that the regulatory subunits may fine tune Stat3-regulated gene expression. However, transcription of Stat3-regulated genes implicated in LM-PCD, such as Spi2a and cathepsins B and L, was not affected by ablation of p55α/p50α although there was a trend of reduced expression of cathepsin L (Figure 3d). Taken together, these data suggest that p55α/p50α modulate the expression of distinct sets of genes at either the transcriptional or post-transcriptional level during mammary gland involution.

a p55α⁺/⁺/p50α⁺/⁺ p55α⁻/⁻/p50α⁻/⁻

b p55α⁺/⁺/p50α⁺/⁺ p55α⁻/⁻/p50α⁻/⁻

c

d

e 24h Inv

c-C3/Hoechst

f
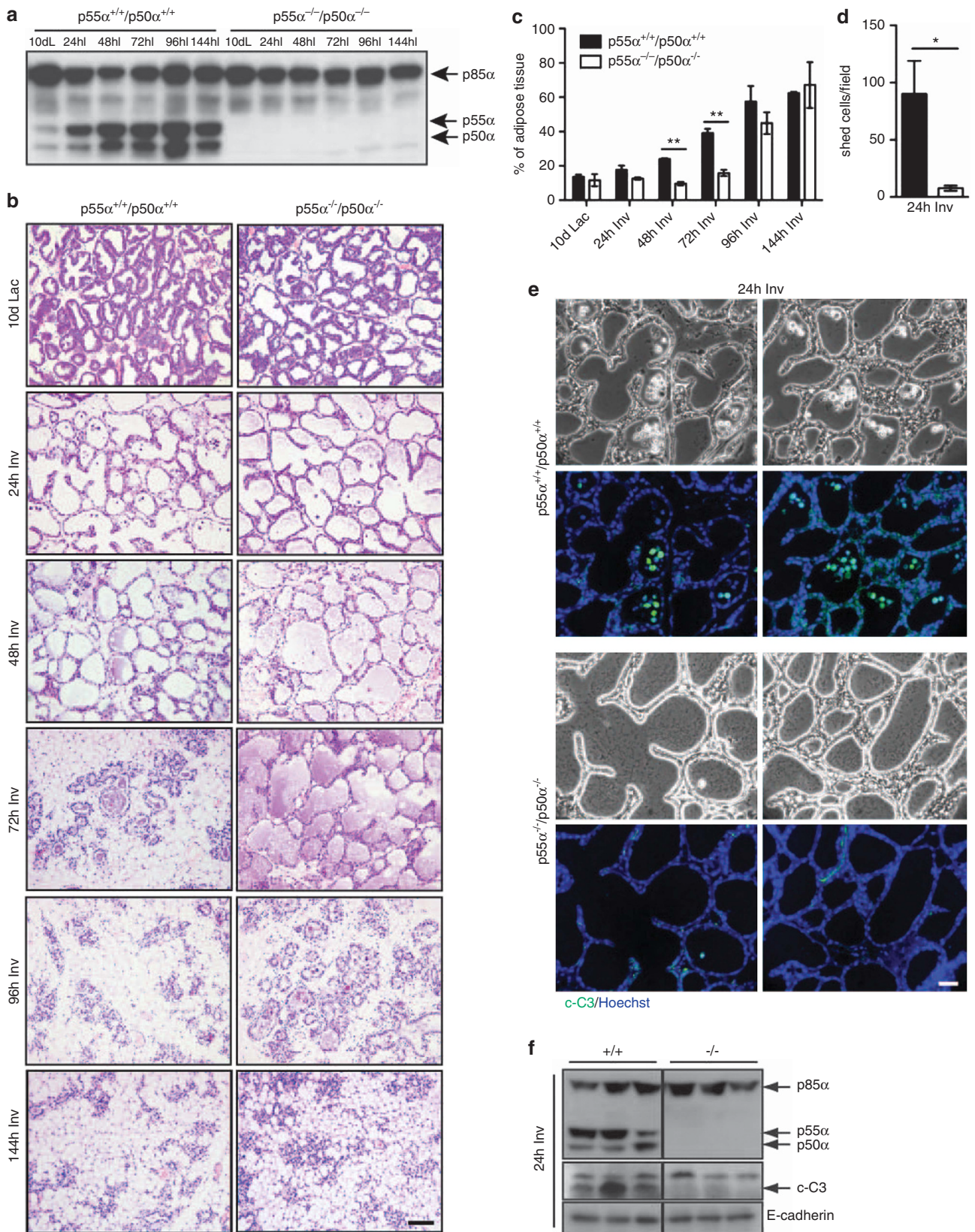
Cathepsin L is an important mediator of mammary gland involution. The specific regulation of cathepsin L downstream of the small regulatory subunits p55α/p50α points to an important role for this lysosomal enzyme in cell death. To address this function directly, we investigated involution at various time points in cathepsin L null mice. Involution was markedly delayed with a threefold reduction in the extent of tissue remodeling observed in ctsl$^{-/-}$ mammary glands at 72-h involution as measured by the area occupied by adipocytes (Figures 4a–c). In addition, perilipin staining of mammary glands at 72 h of involution highlights the delayed reappearance of the adipocytes in the ctsl$^{-/-}$ glands when compared with the controls (Figure 4d).

Discussion

Of the three subunits encoded by the *pi3kr1* gene, p85α has been implicated in a plethora of functions, which may be either PI3K dependent or independent and are exerted mainly through interaction with several binding partners in different contexts.[18] The role of the smaller p55α/p50α subunits is, however, still obscure. The only clearly defined function for p55α/p50α was revealed by their genetic deletion, which resulted in increased insulin sensitivity, demonstrating a role for the small subunits in insulin signaling, particularly in glucose and lipid metabolism.[6] It has been hypothesized that their unique N-termini may target these subunits to different compartments of the cell, thus allowing for localized PI3K-dependent signaling events. For example, the p55α N-terminus has been shown to interact with tubulin, thus localizing this subunit to the microtubule network.[7]

Here we show that p55α/p50α, specifically upregulated at the onset of involution by Stat3, have a fundamental role *in vivo* by regulating mammary gland involution. In the absence of the small subunits, mammary gland involution is substantially delayed, with a severe effect on the levels of cell death during the early stages of this process (Figure 1). Surprisingly, p55α/p50α affect cell death independently of PI3K signaling, as phosphorylation of Akt and its downstream targets are largely unaffected in knockout tissue (Supplementary Figure 1).

One mechanism by which the subunits influence cell death, which occurs by LM-PCD, is by upregulating levels of the lysosomal protease cathepsin L (Figure 2). Furthermore, we provide evidence that reduced activity of cathepsin L can at least partially account for the delay in involution observed in the p55α/p50α mice, as complete depletion of this lysosomal protease, as observed in *ctsl*$^{-/-}$ mice, is sufficient to delay mammary gland involution (Figure 4).

The upregulation of cathepsin L does not seem to occur directly through transcriptional regulation, as the mRNA levels of cathepsin L are not significantly reduced in the *p55α*$^{-/-}$/*p50α*$^{-/-}$ mice (Figure 3d). Post-transcriptional regulation of cathepsin L has not been investigated and could occur by alterations in mRNA stability or post-translational delivery to the lysosomal compartment.

Interestingly, however, we could detect p55α/p50α, as well as p85α, in the nuclear compartment of mammary tissue and mammary cell lines (Figures 3a and b). There is some evidence in the literature for nuclear localization of particular regulatory subunits of PI3K. For example, p85α has been shown to localize to the nuclei of both PC12 cells upon Haloperidol treatment[16] and C6 glial cells cultured in serum-free medium.[17] More recently, interaction of p85α or p85β with XBP-1s has been shown to increase nuclear localization of XBP-1s and transcriptional regulation of the UPR.[4,5] Furthermore, both p85α and p85β have been shown to be present in nuclear preparations of mouse embryonic fibroblasts.[4] Our finding that p55α/p50α localize to the nuclei of mammary cells and associate with chromatin is the first demonstration of a potential nuclear function for these smaller subunits. This notion is supported by our microarray analysis demonstrating that gene expression during involution is modulated by depletion of p55α/p50α suggesting a role in transcriptional regulation, which could be mediated by influencing the activity of other transcription factors, such as Stat3 (Figure 3c and Supplementary Tables). However, further investigation is required to address the specific mechanism.

Mammary gland involution is associated with a marked upregulation of the APR and inflammatory genes.[11,14,19] The APR is a component of the innate immune system and the first mechanism of defense against disease, aimed at minimizing tissue damage while promoting repair. We have recently demonstrated some of the APR genes to be transcriptional targets of Stat3 in the mammary gland,[10] where they may act to ensure efficient tissue remodeling.

An initial comparison of the most markedly p55α/p50α-regulated genes reveals that many downregulated targets are also substantially downregulated in the absence of Stat3. Similarly, many of the genes upregulated in the 24 h p55α/p50α-depleted mammary gland are also upregulated in the *Stat3*$^{-/-}$ tissue (Supplementary Table 3). These correlations indicate that a set of Stat3-regulated involution target genes are also regulated via p55α/p50α, suggesting that these subunits modulate the Stat3 signal. Intriguingly, however, a small number of genes are upregulated in the p55α$^{-/-}$/p50α$^{-/-}$ but downregulated in the *Stat3*$^{-/-}$ glands, indicating positive

---

Figure 1 p55α/p50α regulate cell death *in vivo*. (**a**) Immunoblot showing the complete deletion of p55α and p50α with retention of p85α in the *p55α*$^{-/-}$/*p50α*$^{-/-}$ mammary glands throughout involution. dL, days of lactation; hI, hours of involution. (**b**) Delay of mammary gland involution in *p55α*$^{-/-}$/*p50α*$^{-/-}$ mice, compared with *p55α*$^{+/+}$/*p50α*$^{+/+}$ control mice, shown by hematoxylin and eosin (H&E)-stained sections. Scale bar, 200 μm. (**c**) Quantification of the area occupied by adipocytes, showing a significant difference in the percentage of adipose tissue at both 48- and 72-h involution. The values represent means ± S.E.M. of two to four individual mice. (**d**) Quantification of luminal shed cells as detected in the H&E sections of 24-h involution samples. The values represent means ± S.E.M. of three individual mice, with four fields per mouse counted. Black and white bars represent *p55α*$^{+/+}$/*p50α*$^{+/+}$ and *p55α*$^{-/-}$/*p50α*$^{-/-}$ glands, respectively. Lac, lactation; Inv, involution. (**e**) Immunohistochemical analysis of the occurrence of cleaved caspase 3 in *p55α*$^{-/-}$/*p50α*$^{-/-}$ and control *p55α*$^{+/+}$/*p50α*$^{+/+}$ mice at 24-h involution. Cleaved caspase-3 (c-C3)-positive shed cells can only be detected in the control mice. Scale bar, 100 μm. (*$P < 0.05$, **$P < 0.01$, as determined by Student's *t*-test). (**f**) Immunoblot of cleaved-caspase 3 (c-C3) in control (+/+) and *p55α*$^{-/-}$/*p50α*$^{-/-}$ mice (−/−) at 24-h involution. E-cadherin is shown as loading control
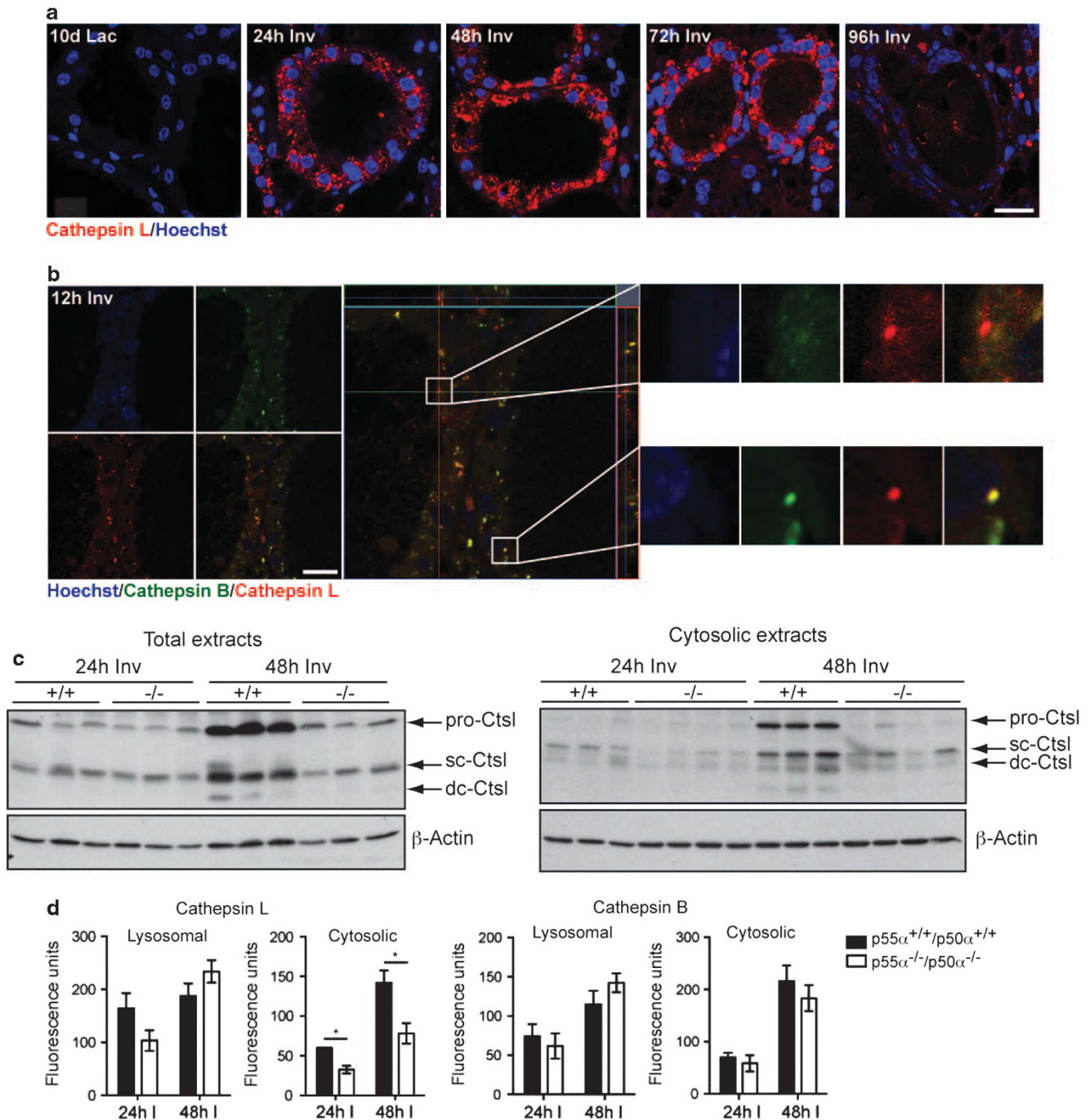
Figure 2 p55α/p50α regulate cathepsin L expression and cytosolic activity. (**a**) Rapid upregulation of cathepsin L at the onset of involution. Immunohistochemical analysis of cathepsin L (red) in control mice. 10d Lac, 10 days lactation; 24, 48, 72, 96 h Inv, hours of involution. Nuclei are stained with Hoechst. Scale bar, 20 μm. (**b**) Vesicles containing cathepsin L (red) but not cathepsin B (green) are shown by immunohistochemistry on 12-h involution control samples. Insets of an example of a vesicle containing only cathepsin L and one containing both cathepsin L and B are shown on the right side. Nuclei are stained with Hoechst. Scale bar, 20 μm. (**c**) Left, immunoblot showing decreased levels of cathepsin L (Ctsl) in the *p55α*⁻/⁻/*p50α*⁻/⁻ (−/−) mice as compared with control *p55α*⁺/⁺/*p50α*⁺/⁺ (+/+) mice. Three individual mice are shown per genotype at both 24-h involution and 48-h involution. Right, immunoblot of cytosolic extracts of three control and four *p55α*⁻/⁻/*p50α*⁻/⁻ mammary glands (sc, single chain; dc, heavy chain of the double-chain form; both the single-chain and the double-chain form are active). β-Actin is shown as loading control. (**d**) Reduced cytosolic activity of cathepsin L at 24- and 48-h involution in *p55α*⁻/⁻/*p50α*⁻/⁻ glands when compared with controls, as opposed to unchanged cathepsin B activity shown by subcellular fractionation and subsequent cathepsin activity measurement. All values are means ± S.E.M. of at least three independent biological repeats. (*$P < 0.05$, as determined by Student's *t*-test)

regulation by Stat3 and negative regulation by p55α/p50α. The reason for this is not clear but may be a mechanism for fine tuning the amplitude of the Stat3 response.

Our previous work demonstrated that Stat3 regulates LM-PCD[12] and induces expression of p55α and p50α.[13] In other work (Pensa *et al.*, unpublished), we have shown that
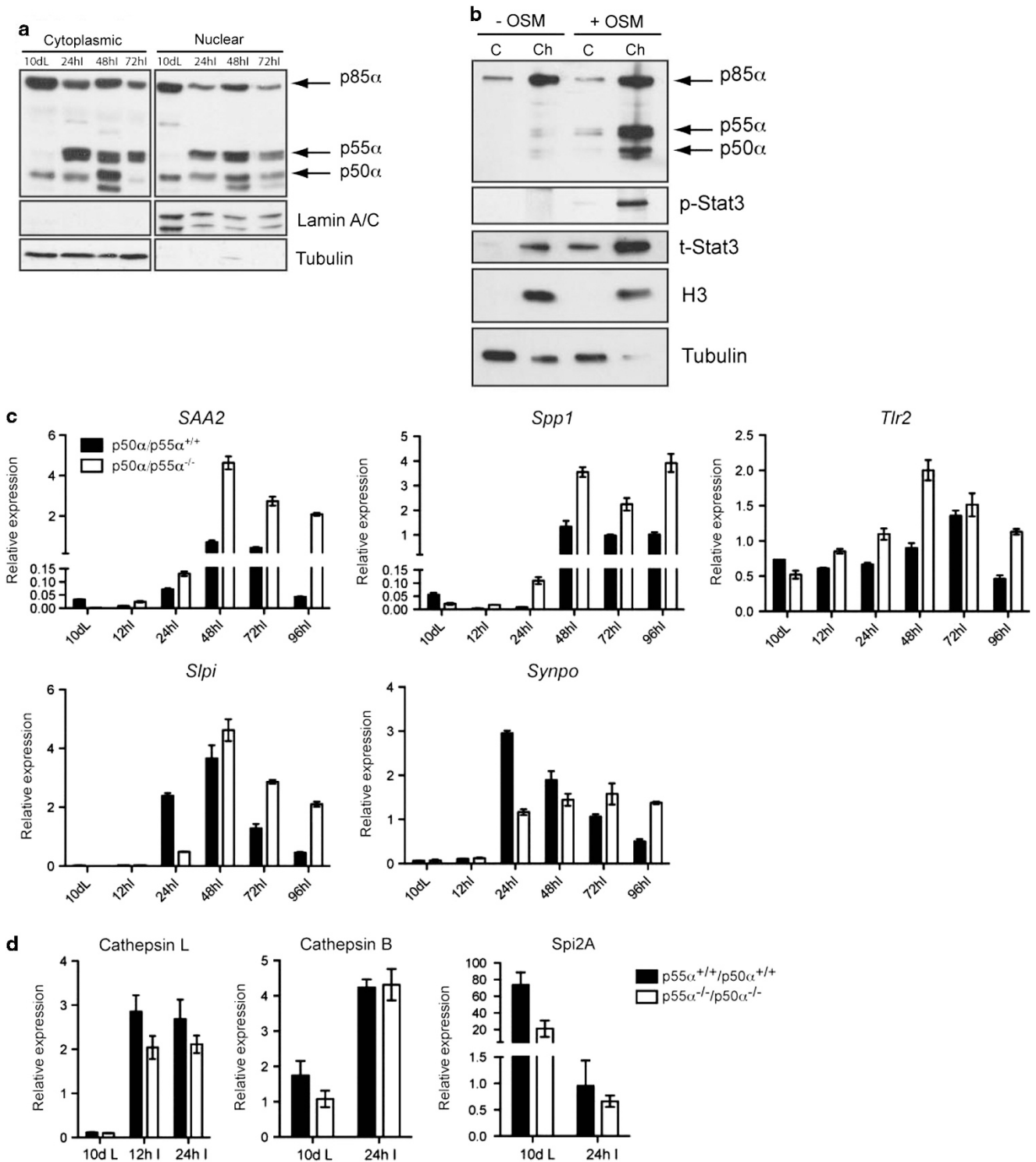
Figure 3 p50α and p55α localize to the nuclei of mammary glands during involution and regulate transcription of a subset of genes. (**a**) Nuclear/cytosolic fractionation of mammary glands showing both cytosolic and nuclear localization of p50α, p55α and p85α. Lamin A/C and tubulin are shown as loading and purity controls for the nuclear and cytosolic fraction, respectively. (**b**) Chromatin-enriched extracts of EpH4 mammary epithelial cells treated with vehicle (− OSM) or OSM (+ OSM) showing the presence of phospho-Stat3 (p-Stat3) and p55α/p50α mainly in the chromatin-enriched fraction (ch) of the OSM-treated cells as opposed to the cytosolic (C) fraction, whereas p85α is present on chromatin also in the control cells. t-Stat3, total Stat3. Histone H3 (H3) is shown as chromatin marker, whereas tubulin shows the cytosolic fraction. Notably, tubulin contamination in the chromatin fraction of the OSM-treated cells is almost undetectable. (**c**) Quantitative real-time PCR relative to *cyclophilin a* of the following genes: *SAA2*, serum amyloid A 2; *Spp1*, secreted phosphoprotein 1; *Tlr2*, Toll-like receptor 2; *Slpi*, secretory leukocyte protease inhibitor; *Synpo*, synaptopodin. All results are means ± S.E.M. for three independent measurements and are representative of two independent biological repeats. (**d**) Quantitative real-time PCR relative to *cyclophilin a* of *Cathepsin L* and *B* and *Spi2A* expression at the indicated time points of mammary gland involution showing a decreased, although not significant, expression of cathepsin L in the $p55α^{-/-}/p50α^{-/-}$ glands as compared with the controls. Results are means ± S.E.M. for at least four independent biological repeats
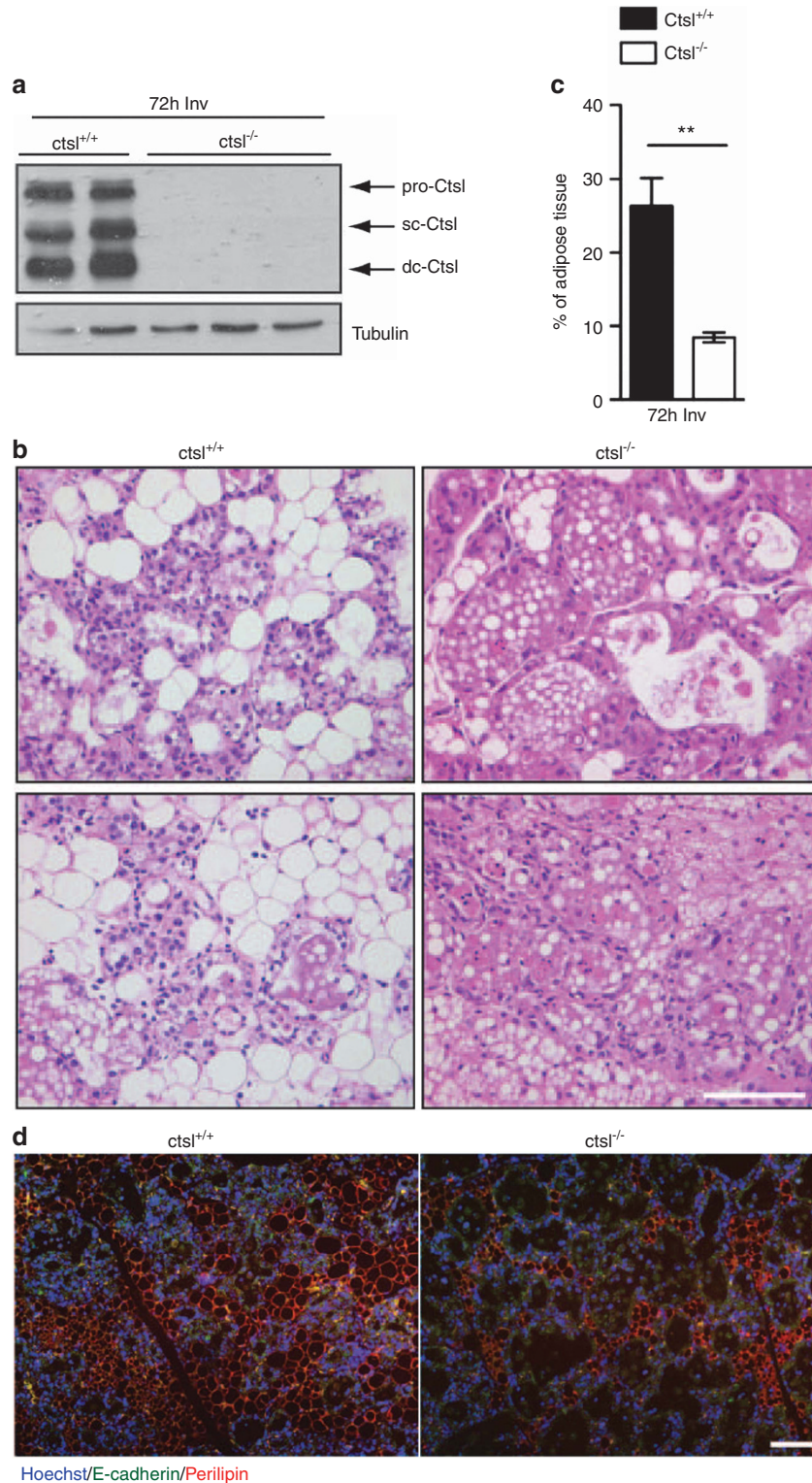
Figure 4 Cathepsin L is an important mediator of mammary gland involution. (**a**) Immunoblot showing the complete deletion of cathepsin L in *cathepsin L*$^{-/-}$ (ctsl$^{-/-}$) glands compared with the controls (ctsl$^{+/+}$) at 72-h involution. Tubulin is shown as loading control. (**b**) H&E sections and (**c**) quantification of the percentage of area occupied by adipocytes at 72-h involution clearly show the delay in involution in ctsl$^{-/-}$ mice compared with the controls. Quantification has been performed on two and three independent biological repeats for the control and the ctsl$^{-/-}$ mice, respectively. All values are means ± S.E.M. (**P < 0.01, as determined by Student's *t*-test; scale bar, 100 μm). (**d**) Immunohistochemical analysis of the adipocytes (stained with perilipin, red) and epithelium (stained with E-cadherin, green) in 72 h of involution samples. Nuclei are stained with Hoechst. Scale bar, 100 μm

p55α and p50α regulate the autophagic flux during involution. We propose a novel function for these subunits as key factors in determining the balance of tissue remodeling signals and cell death in the physiological context of mammary gland involution. This balance between autophagy and cell death is of crucial importance in many different biological processes. Thus, we anticipate that p55α/p50α may be central in cell fate decisions in other systems *in vivo* where they can regulate autophagy and cell death. The APR and the inflammatory response associated with involution have been recently demonstrated to provide a pro-tumorigenic microenvironment in the mammary gland.[20] In addition, deregulation of Stat3 target genes can account for its pro-tumorigenic role as opposed to the pro-cell death role in normal tissue.[21] It would be interesting to investigate if the subunits could be responsible for such a switch in Stat3 function in pathological *versus* physiological conditions. The observation that p55α/p50α show higher levels in low grade as compared with aggressive neuroblastomas[22] and that transcription of p55α/p50α by Stat3 switches MEFs from a pro-survival to an anti-survival response to leukemia inhibitory factor (LIF)[23] would support this hypothesis.

Materials and Methods

Animal husbandry. *p55α/p50α* and *ctsl* null mice have been generated previously (Chen *et al.*[6] and Roth *et al.*,[24] respectively). C57BL/6 mice were purchased from Harlan Labs (Indianapolis, IN, USA). The mice were bred in regular cages with food and water *ad libitum*. Virgin female mice, 8–14 weeks old, were mated and males were subsequently removed before birth to avoid second pregnancies. Dams were killed at indicated time points. For involution studies, pups were removed at 10 days of lactation. Unless otherwise stated, at least three mice were used for each time point in every experiment. All animals were treated according to local ethical committee and the UK Home Office guidelines and killed through CO_2 asphyxiation or dislocation of the neck.

Assessment of delayed involution *in vivo*. To quantify the delay of mammary gland involution, the area occupied by adipocytes was assessed by analysis of hematoxylin- and eosin-stained mammary gland sections using ImageJ software (U.S. National Institutes of Health, Bethesda, MD, USA).

Hematoxylin and eosin staining. Hematoxylin and eosin staining was carried out as previously described.[25]

Adipocyte isolation. Pairs of cervical and abdominal (minus lymph nodes) glands were extracted, pooled and minced manually and a small amount of tissue was retained for extraction of total protein. The remaining material was digested for 1 h in 2.5 ml 3 mg/ml type II collagenase at 37 °C with shaking (200 r.p.m.), followed by filtration (filter cap 100 μm pore size; BD Biosciences, San Jose, CA, USA) and centrifugation at low speed (1300 r.p.m.). After centrifugation, mature adipocytes on the surface of the digestion mixture were removed by pipette. 'Undigested' tissue (material that failed to pass through the filter mesh) containing epithelium, stroma and some undigested fat, was retained for analysis. Pelleted material (1300 r.p.m.), expected to contain pre-adipocytes, was also similarly retained.

Lysosomal subcellular fractionation. Lysosomal crude extracts were obtained as previously described.[3] Briefly, lymph node divested number four glands were homogenized in a tight-fitting handheld homogenizer in 1 ml of subcellular fractionation buffer (HEPES-KOH 20 mM, sucrose 250 mM, KCl 10 mM, MgCl₂ 1.5 mM, EDTA 1 mM, EGTA 1 mM, dithiothreitol 8 mM, Pefabloc 1 mM (Sigma Aldrich, St. Louis, MO, USA), at pH 7.5). Debris and nuclei were pelleted at 750 g (3500 r.p.m., Optima L-100 XP Ultracentrifuge, 4 °C, BeckmanCoulter, Brea, CA, USA) for 12 min. The supernatant was spun at 10 000 g (12 900 r.p.m.) for 35 min to pellet lysosomes and other organelles. The pellet was rinsed and collected in 300 μl subcellular fractionation buffer as lysosomal fraction. The supernatant, containing cytosolic and extracellular

components, was cleared of microsomes by an additional spin at 100 000 g (40 000 r.p.m.) for 1 h and collected as cytosolic fraction. Three cycles of freezing and thawing were used to disrupt the organelles.

Cathepsins B and L activity. To measure lysosomal and cytosolic cathepsin activity, subcellular fractionation was carried out as described earlier. Protein levels were assessed with the BCA Protein Assay (Thermo Fisher Scientific, Waltham, MA, USA) and equal amounts of protein (4 μg) were added to a total of 200 μl cathepsin reaction buffer (sodium acetate 50 mM, EDTA 8 mM, dithiothreitol 8 mM and Pefabloc subcellular fractionation buffer 1 mM, at pH 6). Cathepsin B + L activity was measured after incubation (15 min, 37 °C) with the fluorescent substrate Z- Phe-Arg-AMC (50 μM; Merk Millipore, Darmstadt, Germany) in a Synergy HT Multi-Detection Microplate Reader (excitation 380 nM, emission 442 nM; Bio-TEK, Winooski, VT, USA). In parallel, a sample with added cathepsin B inhibitor CA-074 (5 μM; Peptanova, Sandhausen, Germany) was measured to determine cathepsin L activity. The cathepsin B activity measurement was detracted from the difference between readings.

Cytosolic-nuclear fractionation. Cytosolic and nuclear fractions were prepared as following: frozen tissue powder was resuspended in three pellet volumes of cold buffer A (20 mM HEPES, pH 7.0, 0.15 mM EDTA, 0.015 mM EGTA, 10 mM KCl, 1 mM phenylmethylsulfonyl fluoride, 20 mM NaF, 1 mM sodium pyrophosphate, 1 mM sodium orthovanadate, 1% Nonidet P-40, and protease inhibitors cocktail (Sigma Aldrich)). The homogenate was centrifuged at 500 × g for 5 min. The supernatant corresponds to the cytosolic fraction. The nuclear pellet was resuspended in five pellet volumes of cold buffer B (10 mM HEPES, pH 8.0, 0.1 mM EDTA, 1 mM phenylmethylsulfonyl fluoride, 20 mM NaF, 1 mM sodium pyrophosphate, 1 mM sodium orthovanadate, 25% glycerol, 0.1 M NaCl and protease inhibitors cocktail). After centrifugation, the nuclei were resuspended in two pellet volumes of hypertonic cold buffer C (10 mM HEPES, pH 8.0, 0.1 mM EDTA, 1 mM phenylmethylsulfonyl fluoride, 20 mM NaF, 1 mM sodium pyrophosphate, 1 mM sodium orthovanadate, 25% glycerol, 0.4 M NaCl and protease inhibitors cocktail) and were incubated for 30 min at 4 °C in a rotating wheel and nuclear debris were removed by centrifugation at 900 × g for 20 min at 4 °C.

Small-scale chromatin-cytosolic fractionation. EpH4 cells were grown in DMEM (Life Technologies, Carlsbad, CA, USA) containing 10% fetal calf serum (Sigma Aldrich). To isolate the chromatin, cells were plated in 10 cm dishes, treated with OSM for 24 h, crosslinked and quenched as described before.[26] Cells were washed with PBS, centrifuged and the cell pellet was resuspended in buffer A (10 mM HEPES (pH 7.9), 10 mM KCl, 1.5 mM MgCl₂, 0.34 M sucrose, 10% glycerol, 1 mM dithiothreitol and protease inhibitor cocktail (Sigma Aldrich)). Triton X-100 was added (0.1% final concentration), the cells were incubated on ice for 10 min, and nuclei were collected by centrifugation (5 min, 1300 × g, 4 °C). The supernatant constitutes the cytosolic fraction. The nuclei were washed once in buffer A and lysed for 30 min in buffer B (3 mM EDTA, 0.2 mM EGTA, 1 mM dithiothreitol and protease inhibitor cocktail), and insoluble chromatin and soluble fraction were separated by centrifugation (5 min, 1700 × g, 4 °C). The chromatin fraction was washed five times with buffer B. On the last wash, sonication was performed for 30 s. After centrifugation at 4000 r.p.m. for 5 min at 4 °C, the chromatin pellet was resuspended in 55 μl 1X DNase I Buffer + 5 μl DNase (Promega, Madison, WI, USA), incubated at 37 °C for 30–60 min and boiled 15 min in sodium dodecyl sulfate loading buffer.

Quantitative real-time PCR. RNA extraction, complementary DNA synthesis and quantitative real-time PCR were carried out as previously described.[25] Primers used were: *cyclophilin A* (housekeeping gene) forward, 5′-CCTTGGGC CGCGTCTCCTT-3′, reverse, 5′-CACCCTGGCACATGAATCCTG-3′; *cathepsin B* forward, 5′-TCCTTGATCCTTCTTTCTTGCC-3′, reverse, 5′-ACAGTGCCACAC AGCTTCTTC-3′; *cathepsin L* forward, 5′-ATCAAACCTTTAGTGCAGAGTG-3′, reverse, 5′-CTGTATTCCCCGTTGTGTAGC-3′; *Spi2A* forward, 5′-TTTCCAG CAACCTCTCAAGGC-3′, reverse, 5′-CTGGGTGTGATTGCCCACATA-3′. *Saa2* forward, 5′-TGGCTGGAAAGATGGAGACAA-3′, reverse, 5′-AAAGCTCTCTCTTG CATCACTG-3′; *Spp1* forward, 5′-AGCAAGAAACTCTTCCAAGCAA-3′, reverse, 5′-GTGAGATTCGTCAGATTCATCCG-3′; *Synpo* forward, 5′-GCTCATTGACATG CAGCCTA-3′, reverse, 5′-GCCTTCTCTCCAAACTGTCG-3′; *Tlr2* forward, 5′-GCAAACGCTGTTCTGCTCAG-3′, reverse, 5′-AGGCGTCTCCCTCTATTG TATT-3′. Primers were designed using the PrimerBank website (http://pga.mgh. harvard.edu/primerbank/).

Immunoblotting. Sample preparation and immunoblotting were carried out as previously described.[25] The following antibodies from Cell Signalling Technologies (Danvers, MA, USA) were used: anti-phospho-Stat3 (Tyr705: 9131), anti-total-Stat3 (9132), anti-phospho-Akt (Ser473: 9271), anti-total-Akt (9272), anti-phospho-Gsk3β (9331), anti-GSK3β (9315), anti-Akt1 (2967), anti-Akt2 (2964), anti-Akt3 (4059) and anti-lamin A/C (2032). The following antibodies from Abcam (Cambridge, UK) were used: anti-cathepsin B (ab33538), anti-Lamp2 (ab13524), anti-tubulin (ab6160) and anti-β-actin (ab8227). The following antibodies from Santa Cruz Biotechnology (Santa Cruz, CA, USA) were used: anti-C/ebpα (sc-61), anti-histone H3 (sc8654), anti-Bax (sc-7480), anti-Bcl-2 (sc7382) and anti-Bcl-xL (sc-634). Other commercial antibodies used were: anti-cathepsin L (MAB9521), anti-cathepsin L (AF1515, used for the immunodetection of cathepsin L in the cathepsin L knockout and control glands) and anti-Bid (MB860) from R&D Systems (Minneapolis, MN, USA), anti-pan-p85 (Merk Millipore, 06-496, also detects p50α/p55α subunits), anti-cytochrome c (65981A) and anti-E-cadherin (610182) from BD Biosciences. All antibodies were used at a standard dilution of 1 : 1,000. Secondary horseradish peroxidase-conjugated antibodies were purchased from Dako (Glostrup, Denmark).

Immunohistochemistry. Tissue sections were prepared as previously described.[25] For assessment of cathepsin localization on tissue sections, the tissue was permeabilized with 0.1% saponin (Sigma Aldrich) in PBS and blocked in 10% normal goat serum (Dako) in PBS, 0.01% saponin. The pictures of c-C3 were acquired on a Zeiss Axioplan 2 microscope (Zeiss, Jena, Germany). All the other pictures were acquired on a Zeiss LSM 700 confocal microscope. Z-stacks for the cathepsins B and L costaining were carried out on at least five z-stacks from two independent biological replicates with at least 10 cross-sections for every sample. Primary antibodies used were: rat anti-cathepsin L (R&D Systems; MAB9521, 1 : 200), rabbit anti-cathepsin B (Abcam; 1 : 100), mouse anti-E-cadherin (BD Biosciences; 610182, 1 : 500), rabbit anti-perilipin (Cell Signalling Technologies; 3470, 1 : 200) and rabbit anti-cleaved caspase 3 (Cell Signalling Technologies; 9661, 1 : 100). Secondary antibodies used were Alexa Fluor 488 goat-anti-rabbit-IgG (Life Technologies; 1 : 500) Cy3 goat-anti-rabbit (Life Technologies; 1 : 500) and Cy3 goat-anti-rat-IgG (Life Technologies; 1 : 500). Nuclei were counterstained with Hoechst 33342 (Sigma Aldrich; 1 : 1000).

Statistical analysis. Every experiment was carried out with at least three independent biological samples, unless otherwise stated. Where appropriate, statistical significance was assessed with Student's t-test.

Conflict of Interest

The authors declare no conflict of interest.

1. Vanhaesebroeck B, Ali K, Bilancio A, Geering B, Foukas LC. Signalling by PI3K isoforms: insights from gene-targeted mice. *Trends Biochem Sci* 2005; **30**: 194–204.
2. Mellor P, Furber LA, Nyarko JN, Anderson DH. Multiple roles for the p85alpha isoform in the regulation and function of PI3K signalling and receptor trafficking. *Biochem J* 2012; **441**: 23–37.
3. Chagpar RB, Links PH, Pastor MC, Furber LA, Hawrysh AD, Chamberlain MD et al. Direct positive regulation of PTEN by the p85 subunit of phosphatidylinositol 3-kinase. *Proc Natl Acad Sci USA* 2010; **107**: 5471–5476.
4. Park SW, Zhou Y, Lee J, Lu A, Sun C, Chung J et al. The regulatory subunits of PI3K, p85alpha and p85beta, interact with XBP-1 and increase its nuclear translocation. *Nat Med* 2010; **16**: 429–437.
5. Winnay JN, Boucher J, Mori MA, Ueki K, Kahn CR. A regulatory subunit of phosphoinositide 3-kinase increases the nuclear accumulation of X-box-binding protein-1 to modulate the unfolded protein response. *Nat Med* 2010; **16**: 438–445.
6. Chen D, Mauvais-Jarvis F, Bluher M, Fisher SJ, Jozsi A, Goodyear LJ et al. p50alpha/p55alpha phosphoinositide 3-kinase knockout mice exhibit enhanced insulin sensitivity. *Mol Cell Biol* 2004; **24**: 320–329.
7. Inukai K, Funaki M, Nawano M, Katagiri H, Ogihara T, Anai M et al. The N-terminal 34 residues of the 55 kDa regulatory subunits of phosphoinositide 3-kinase interact with tubulin. *Biochem J* 2000; **346**(Pt 2): 483–489.
8. Watson CJ. Post-lactational mammary gland regression: molecular basis and implications for breast cancer. *Expert Rev Mol Med* 2006; **8**: 1–15.
9. Chapman RS, Lourenco PC, Tonner E, Flint DJ, Selbert S, Takeda K et al. Suppression of epithelial apoptosis and delayed mammary gland involution in mice with a conditional knockout of Stat3. *Genes Dev* 1999; **13**: 2604–2616.
10. Hughes K, Wickenden JA, Allen JE, Watson CJ. Conditional deletion of Stat3 in mammary epithelium impairs the acute phase response and modulates immune cell numbers during post-lactational regression. *J Pathol* 2012; **227**: 106–117.
11. Stein T, Morris JS, Davies CR, Weber-Hall SJ, Duffy MA, Heath VJ et al. Involution of the mouse mammary gland is associated with an immune cascade and an acute-phase response, involving LBP, CD14 and STAT3. *Breast Cancer Res* 2004; **6**: R75–R91.
12. Kreuzaler PA, Staniszewska AD, Li W, Omidvar N, Kedjouar B, Turkson J et al. Stat3 controls lysosomal-mediated cell death in vivo. *Nat Cell Biol* 2011; **13**: 303–309.
13. Abell K, Bilancio A, Clarkson RW, Tiffen PG, Altaparmakov AI, Burdon TG et al. Stat3-induced apoptosis requires a molecular switch in PI(3)K subunit composition. *Nat Cell Biol* 2005; **7**: 392–398.
14. Clarkson RW, Boland MP, Kritikou EA, Lee JM, Freeman TC, Tiffen PG et al. The genes induced by signal transducer and activators of transcription (STAT)3 and STAT5 in mammary epithelial cells define the roles of these STATs in mammary development. *Mol Endocrinol* 2006; **20**: 675–685.
15. Burke MA, Hutter D, Reshamwala RP, Knepper JE. Cathepsin L plays an active role in involution of the mouse mammary gland. *Dev Dyn* 2003; **227**: 315–322.
16. Dai Y, Wei Z, Sephton CF, Zhang D, Anderson DH, Mousseau DD. Haloperidol induces the nuclear translocation of phosphatidylinositol 3'-kinase to disrupt Akt phosphorylation in PC12 cells. *J Psychiatry Neurosci* 2007; **32**: 323–330.
17. Sephton CF, Mousseau DD. Dephosphorylation of Akt in C6 cells grown in serum-free conditions corresponds with redistribution of p85/PI3K to the nucleus. *J Neurosci Res* 2008; **86**: 675–682.
18. Mellor P, Furber LA, Nyarko JN, Anderson DH. Multiple roles for the p85alpha isoform in the regulation and function of PI3K signalling and receptor trafficking. *Biochem J* 2012; **441**: 23–37.
19. Pensa S, Watson CJ, Poli V. Stat3 and the inflammation/acute phase response in involution and breast cancer. *J Mammary Gland Biol Neoplasia* 2009; **14**: 121–129.
20. Lyons TR, O'Brien J, Borges VF, Conklin MW, Keely PJ, Eliceiri KW et al. Postpartum mammary gland involution drives progression of ductal carcinoma in situ through collagen and COX-2. *Nat Med* 2011; **17**: 1109–1115.
21. Resemann HK, Watson CJ, Lloyd-Lewis B. The Stat3 paradox: a killer and an oncogene. *Mol Cell Endocrinol* 2014; **382**: 603–611.
22. Fransson S, Kogner P, Martinsson T, Ejeskar K. Aggressive neuroblastomas have high p110alpha but low p110delta and p55alpha/p50alpha protein levels compared to low stage neuroblastomas. *J Mol Signal* 2013; **8**: 4.
23. Lu Y, Fukuyama S, Yoshida R, Kobayashi T, Saeki K, Shiraishi H et al. Loss of SOCS3 gene expression converts STAT3 function from anti-apoptotic to pro-apoptotic. *J Biol Chem* 2006; **281**: 36683–36690.
24. Roth W, Deussing J, Botchkarev VA, Pauly-Evers M, Saftig P, Hafner A et al. Cathepsin L deficiency as molecular defect of furless: hyperproliferation of keratinocytes and pertubation of hair follicle cycling. *Faseb J* 2000; **14**: 2075–2086.
25. Khaled WT, Read EK, Nicholson SE, Baxter FO, Brennan AJ, Came PJ et al. The IL-4/IL-13/Stat6 signalling pathway promotes luminal mammary epithelial cell development. *Development* 2007; **134**: 2739–2750.
26. Schmidt D, Wilson MD, Spyrou C, Brown GD, Hadfield J, Odom DT. ChIP-seq: using high-throughput sequencing to discover protein-DNA interactions. *Methods* 2009; **48**: 240–248.

Supplementary Information accompanies this paper on Cell Death and Differentiation website (http://www.nature.com/cdd)